Multimedia Tools and Applications (2019) 78:15909–15928
https://doi.org/10.1007/s11042-018-6967-4

DLGBD: A directional local gradient based descriptor for face recognition

Nazife Cevik[1] · Taner Cevik[2]

Received: 23 March 2018 / Revised: 18 October 2018 / Accepted: 27 November 2018 /
Published online: 10 December 2018

Abstract

This paper proposes a novel high-performance gradient-based local descriptor that handles the prominent challenges of face recognition such as resistance against rotational, illuminative changes as well as noise effects. One of the novelties this study poses is that, while processing the gradient for each direction, an analysis is done by considering the predecessors of the corresponding pixel as well as the successors at that direction. Furthermore, earlier studies represent these local relationships by encoding them in binary because they consider only the positive and negative intensity changes. However, we propose an alternative way of representation that encodes the relationships between each pixel and its neighbors in a multi-valued logic manner called Directional Local Gradient Based Descriptor (DLGBD). Our method not only considers the variations but also uniformity. A threshold value is defined to identify whether an intensity variation is present in the specified direction. If the intensity change exceeds the threshold value, then it is evaluated as a variation either in positively or negatively depending on the direction of the change. Three states of the relationship between multiple pixels at each direction yield a more discriminative descriptor for face retrieval. Ternary logic is applied to express three states. Ternary values that are calculated at each direction are concatenated and the resulting compound ternary value is replaced with the reference pixel. By this way, a more discriminative face descriptor is achieved which is resistant to noise and challenges in unconstrained environments. Extensive simulations are conducted over benchmark datasets and the performance of DLGBD is compared to the other state-of-the-art methods. As presented by the simulation results, the DLGBD achieves very high discriminating performance as well as providing resistance against rotation and illumination variations.

Keywords Face recognition · Local descriptor · Local pattern · Gradient · Classification · Rotation invariant

✉ Taner Cevik
tanercevik@aydin.edu.tr

Nazife Cevik
nazifecevik@arel.edu.tr

[1] Department of Computer Engineering, Istanbul Arel University, Istanbul, Turkey

[2] Department of Software Engineering, Istanbul Aydin University, Istanbul, Turkey

1 Introduction

Biometrics have been paid significant attention and gained a wide application area during the past decades due to their high discriminative performance in a number of fields such as surveillance, identification, human-computer interaction, etc. [14, 65]. Individuals pose biological characteristics also called metrics which separate them from the others [22]. Biometrics deals with these metrics that can be mainly categorized into two groups, physiological and behavioral [23]. Physiological characteristics are related to the shape of the body and most common ones are iris, retina, palm print, fingerprint, etc. Behavioral characteristics also sometimes called behaviometrics [38], i.e. voice, typing rhythm, gait, are related to the behaviors of the individuals. The face has come into prominence as a physiological identifier due to its high discriminative performance and facility of retrieval by remote devices without disturbing people [10, 21].

Face recognition continues to be a research topic that is still in the spotlight and on the agenda with regard to challenges it poses due to the presence of variations in illumination, pose, expression, etc. A great deal of attention has been focused on face recognition due to its challenging nature and wide application areas [27]. Face recognition has mainly based on the idea of classification of images with respect to some features that are specific to individuals. A vast majority of these studies have utilized texture analysis and classification. The texture is the repeating random or regular patterns throughout the image, which characterize the surface of an object or a region [30, 31]. Textures have been widely used as face descriptors to discriminate and retrieve images. Thus, finding high discriminative and low computationally complex descriptors have become a popular point of interest.

Descriptors are mainly categorized as either holistic or local. Methods such as GLCM [15, 16], PCA [25, 55], LDA [11], 2DPCA [59], LLE [50] and VDE [6] concern with the entire image for extracting holistic features, however, local descriptors, namely, LBP [1], LGBP [63], CS-LBP [17], GV-LBP [28], LDP [19], LJBPW [8], PLBP [44], LDGP [4], LPQ [58], LDNP [45, 47], HoG [7], LTP [53], Gabor [33, 60] exploits the local appearance features.

Local descriptors have gained remarkable attention due to their robustness against the prominent challenges of face recognition such as variations in illumination and facial expressions. It is identified that holistic descriptors are more influenced by the aforementioned challenges which as a result impairs their recognition performance. On the other hand, local descriptors pose remarkable recognition rates despite the challenges expressed.

Gabor wavelets, Radon transform [20], Texton learning [26, 56] and LBP are the most prominent methods that have inspired and pioneered many followers [9, 12, 13, 18, 37, 46, 62]. Among this approaches, LBP has remarkably come to the forefront due to its high performance and computationally low complexity [39, 40, 42]. LBP derives micro patterns by considering each pixel's intensity difference relative to its contiguous pixels in its 3×3 neighborhood. Every contiguous pixel in the 3×3 neighborhood contributes as either a binary 1 or 0 to the new value of the reference pixel depending on its own and reference pixel intensity. After completion of the micro-pattern calculation, a histogram representing the distribution of these micro-patterns is created, which takes place as the discriminative feature vector during classification. LBP has found wide application area due to its flexibility to adapt. Thus, a number of successor studies have been proposed [41] to improve and extend the idea of LBP.

In this paper, a gradient-based local descriptor that is robust against the challenges of face recognition is proposed. In contrary to the ordinary methods, while calculating the gradient for

each direction, an analysis is done by considering the predecessors of the corresponding pixel as well as the successors at that direction. Moreover, previous studies represent these local relationships by encoding them in binary because they consider only the positive and negative intensity changes. However, we propose an alternative way of representation that encodes the relationships between each pixel and its neighbors in a multi-valued logic manner. Our method does not only consider the variations but also uniformity. A threshold value is defined to identify whether an intensity variation is present in the specified direction. If the intensity change exceeds the threshold value, then it is evaluated as a variation either in positively or negatively depending on the direction of the change. Three states of the relationship between multiple pixels at each direction yield a more discriminative descriptor for face retrieval. Ternary logic is applied to express three states. Ternary values that are calculated at each direction are concatenated and the resulting compound ternary value is replaced with the reference pixel. By this way, a more discriminative face descriptor is achieved which is resistant to noise and challenges in unconstrained environments. Besides its favorable recognition performance, DLGBD also handles the effects of rotational variances and noise affects very successfully when compared to the state-of-the-art methods.

The rest of this paper is organized as follows. Section 2 briefly reviews the basic LBP and its extensions. Section 3 introduces the proposed local descriptor. Section 4 demonstrates the experimental results and Section 5 concludes the paper.

2 Preliminaries

LBP has gained significant popularity and attention due to its remarkable performance in terms of recognition rate and simplicity [34]. It has influenced many followers and has played a leading role as a source for them, such that, a great deal of research studies has been proposed as an extension of LBP. LBP was firstly produced for texture classification. However, when the high performance it provides was seen, it has been also applied to deduce the relationship between the pixels in the face images [2, 5]. Moreover, a diverse number of LBP variants have been proposed that address the problems in various fields, such as object detection [49, 54], motion and activity analysis [24, 64], biomedical image analysis [35, 36], visual inspection [51], etc.

The original LBP, characterizes the spatial structure of an image by expressing each pixel with a new gray-level value that is calculated relative to the neighboring pixels' gray-level values in a 3×3 neighborhood. A local binary value is formed by concatenating the single-digit binary values that are calculated as the result of magnitude comparison of the reference pixel with each of its neighbors. This, simple, yet efficient local pattern description method, later evolved to a more sophisticated version, which led to multi-resolution analysis and rotation invariance. The successor LBP, operates on a circular neighborhood rather than the square pattern of the predecessor. The neighboring pixels that are settled equally apart from each other on a circle which is centered at the reference pixel (Fig. 1), are considered during pattern description. The coordinates of the neighboring pixel n are defined relative to the reference pixel as$-r \sin(2\pi n/p)$ $r\cos(2\pi n/p)$. Bilinear interpolation is used for regions where the circle does not pass through a certain pixel.

LBP of a reference pixel c, considering its P equally apart neighbors on a circle with radius R, is calculated as in the following:

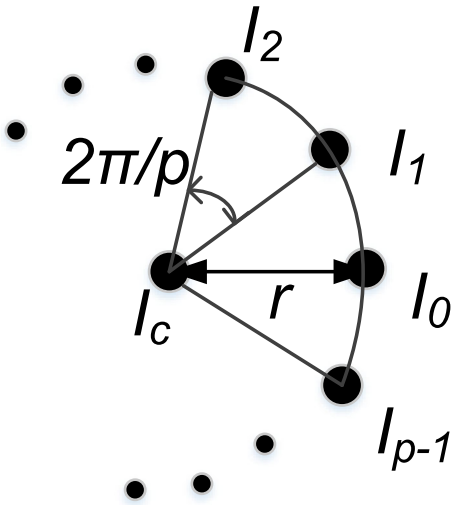

Fig. 1 The p neighbors of the reference pixel I_c on the circle with radius r

$$LBP_{P,R}(c) = \sum_{P=0}^{P-1} s(I_c - I_P)2^p \tag{1}$$

where I_c and I_P denote the intensity values of the reference pixel and the P^{th} neighboring pixel that is considered respectively. The function $s(x)$ identifies the coefficient of the corresponding binary digit and defined as:

$$s(x) = \begin{cases} 1, & if\ x \geq 0 \\ 0, & if\ x < 0 \end{cases} \tag{2}$$

LBP is invariant to monotonic gray-scale changes due to the invariance of the function $s(x)$ against monotonic gray-scale changes [43]. An exemplary demonstration of the basic LBP is given in Fig. 2:

2^p possible different patterns can be calculated. Following the calculation of the LBP values for each pixel, the texture of the image (I_{mxn}) is defined by considering the probability distributions of these LBP values on a histogram, as follows:

$$H(LBP_k) = \sum_{i=1}^{m} \sum_{j=1}^{n} \delta\{k, LBP(i,j)\} \tag{3}$$

where $\delta\{.\}$ denotes the Kroneck product function [3].

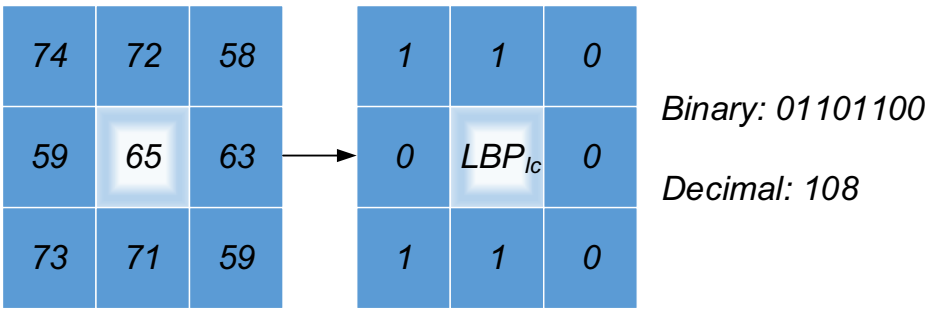

Fig. 2 An exemplary calculation of the basic LBP

The LBP value of each pixel changes when the image is rotated because each digit of the binary pattern corresponds to the result of the comparison of the intensity value of the reference pixel and the neighboring pixel at the specified direction. That is, when the image is rotated, the directional position of the specified neighbor also changes and so the corresponding position in the binary pattern. An extension of the basic LBP is proposed as a rotation invariant version. It has been identified that some of the calculated patterns more information than the others and describe the texture of the images better. Ojala et al. named this subset of 2^p patterns as uniform patterns. An LBP is called uniform if it comprises at most two *0–1* or *1–0* transitions. LBPs such as *10,011,111*, *00010000* are uniform, whereas *10,100,100* and *00110011* are non-uniform.

3 Proposed descriptor - DLGBD

This section presents the proposed local gradient-based descriptor in detail. The first part clarifies the determination of direction-dependent neighbors. The following section describes the nth order local gradient-based information encoding and the last section explains the calculation of the ultimate DLGBD texture descriptor of an image. The overall operational block diagram of DLGBD is illustrated in Fig. 4.

3.1 k-hop directional neighbor extraction

Let, I_{mxn} be a grayscale image where *row* and *col* represent the number of rows and columns respectively. $I_{i,j}$ denotes the intensity value of a pixel in row *(i)*, column *(j)* where $i \in [0,m)$ and $j \in [0,n)$. The coordinates of the top-left-most pixel are *(0,0)*. The column index *j* increases positively in the horizontal direction from left to right, and the row index *i* increases positively downside across the rows. Relations between the pixels are handled in four directions, namely, *0°, 45°, 90°* and *135°*. The local neighborhood that comprises the pixels at most *k*-hop away is represented by N^k. The population of the neighborhood $|N^k|$ differs due to the value of *k* and is calculated as $|N^k| = (2k+1)^k - 1$. The neighbors of a reference pixel $I_{i,j}$ are categorized according to their angular position relative to that pixel. Neighbors of a reference pixel $I_{i,j}$ for $k = 1$ is described as given in Fig. 3:

$$N^1_{0^\circ} = \{I_{i,j-1}, I_{i,j+1}\}, \tag{4}$$

$$N^1_{45^\circ} = \{I_{i+1,j-1}, I_{i-1,j+1}\} \tag{5}$$

$$N^1_{90^\circ} = \{I_{i+1,j}, I_{i-1,j}\} \tag{6}$$

$$N^1_{135^\circ} = \{I_{i+1,j+1}, I_{i-1,j-1}\} \tag{7}$$

$$N^1_{180^\circ} = \{I_{ij+1,j}, I_{i,j-1}\} \tag{8}$$

$$N^1_{225^\circ} = \{I_{i-1,j+1}, I_{i+1,j-1}\} \tag{9}$$

$$N^1_{270^\circ} = \{I_{i-1,j}, I_{i+1,j}\} \tag{10}$$

$$N^1_{315^\circ} = \{I_{i-1,j-1}, I_{i+1,j+1}\} \tag{11}$$

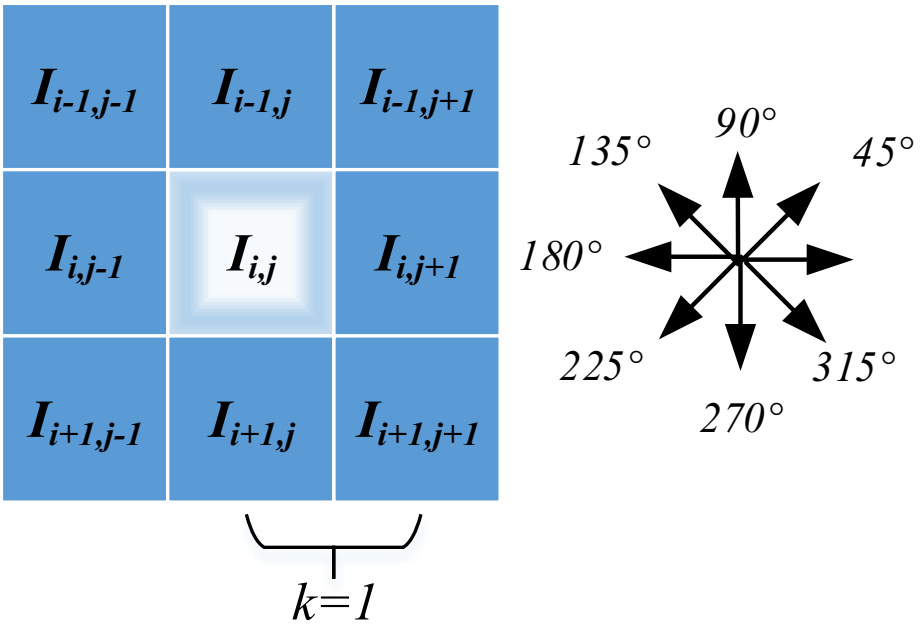

Fig. 3 Directional neighbors of reference pixel $I_{i,j}$ for $k = 1$

where $N^1_{0°}$, $N^1_{45°}$, $N^1_{90°}$, $N^1_{135°}$ $N^1_{180°}$, $N^1_{225°}$, $N^1_{270°}$, $N^1_{315°}$ denote the directional neighbor sets for $\alpha = 0°$, 45°, 90°, 135°, 180°, 225°, 270° and 315° respectively. For $k = 2$, the neighbor sets are defined as in the following which is depicted in Fig. 5 as well.

$$N^2_{0°} = \left\{I'_{i,j-2}, I_{i,j-1}, I_{i,j+1}, I'_{i,j+2}\right\}, \tag{12}$$

where

$$I'_{i,j-2} = mean\left(I_{i-1,j-2}, I_{i,j-2}, I_{i+1,j-2}\right), \tag{13}$$

$$I'_{i,j+2} = mean\left(I_{i-1,j+2}, I_{i,j+2}, I_{i+1,j+2}\right), \tag{14}$$

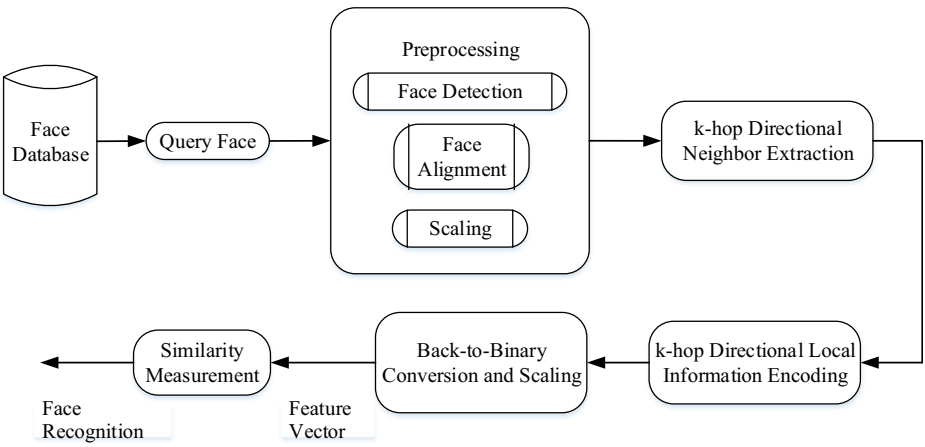

Fig. 4 The block diagram of the complete process

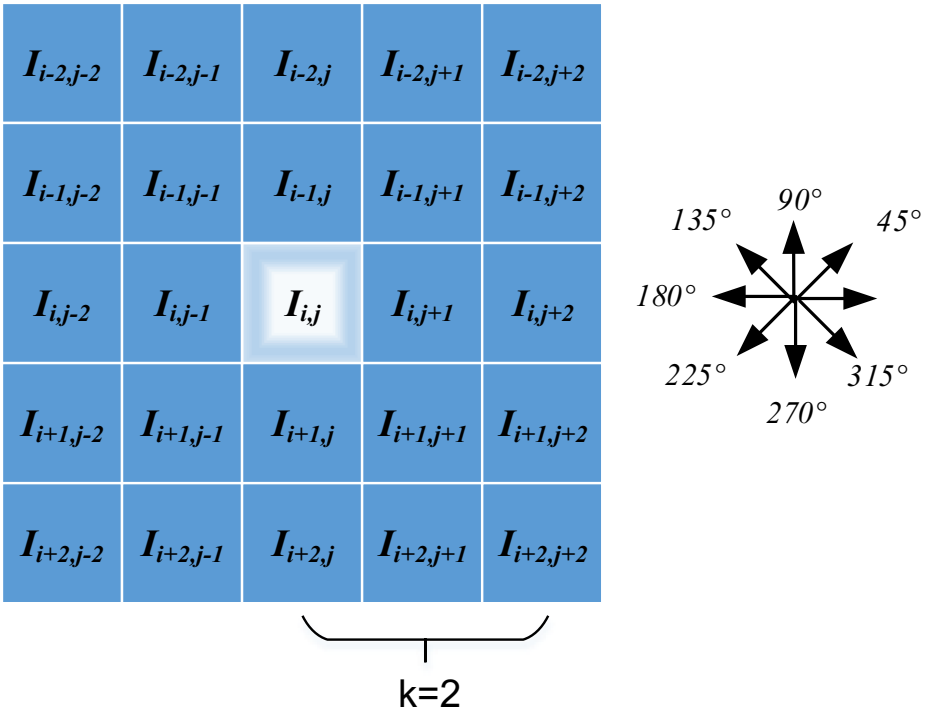

Fig. 5 Directional neighbours of reference pixel $I_{i,j}$ for $k = 2$

$$N^2_{45°} = \{I_{i+2,j-2}, I_{i+1,j-1}, I_{i-1,j+1}, I_{i-2,j+2}\} \tag{15}$$

$$N^2_{90°} = \{I'_{i+2,j}, I_{i+1,j}, I_{i-1,j}, I'_{i-2,j}\}, \tag{16}$$

where

$$I'_{i+2,j} = mean(I_{i-1,j-2}, I_{i,j-2}, I_{i+1,j-2}), \tag{17}$$

$$I'_{i-2,j} = mean(I_{i-1,j+2}, I_{i,j+2}, I_{i+1,j+2}), \tag{18}$$

$$N^2_{135°} = \{I_{i+2,j+2}, I_{i+1,j+1}, I_{i-1,j-1}, I_{i-2,j-2}\} \tag{19}$$

$$N^2_{180°} = \{I'_{i,j+2}, I_{i,j+1}, I_{i,j-1}, I'_{i,j-2}\} \tag{20}$$

$$N^2_{225°} = \{I_{i-2,j+2}, I_{i-1,j+1}, I_{i+1,j-1}, I_{i+2,j-2}\} \tag{21}$$

$$N^2_{270°} = \{I'_{i+2,j}, I_{i+1,j}, I_{i-1,j}, I'_{i-2,j}\} \tag{22}$$

$$N^2_{315°} = \{I_{i-2,j-2}, I_{i+1,j+1}, I_{i-1,j-1}, I_{i+2,j+2}\} \tag{23}$$

As clearly recognized from Eq. (13–14) and Eq. (17–18), when $k >= 2$, mean pixel values $I'_{i,j-2}$, $I'_{i,j+2}$ for $\alpha = 0°$ and $I'_{i+2,j}$, $I'_{i-2,j}$ for $\alpha = 90°$ are calculated by taking into account the predecessor and successor pixels in the specified direction (Fig. 6). Because, four main

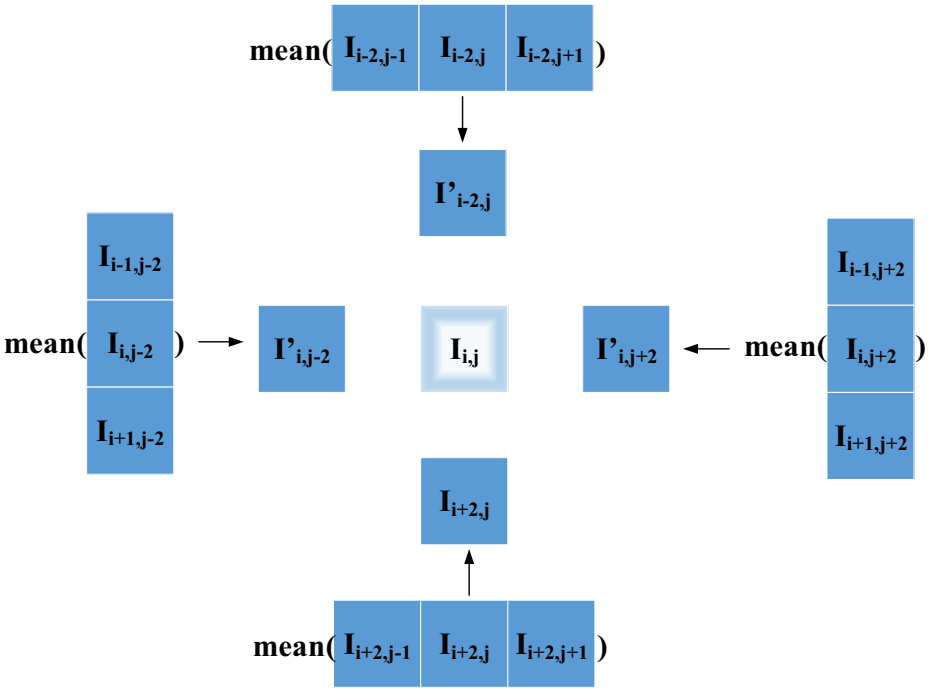

Fig. 6 Definition of neighbors $I'_{i,j-2}$, $I'_{i,j+2}$ for $\alpha = 0°$ and $I'_{i+2,j}$, $I'_{i-2,j}$ for $\alpha = 90°$

directions were identified angularly and these pixels were located on the search lines, thus, they had to be included in an angular pattern.

3.2 k-hop directional local information encoding

In this study, gradient (∇) is used to express the relationship among the pixels. Up to now, research studies have considered only two situations, increasing or decreasing relative pixel shifts. Thus, binary representation has been sufficient to express the two states. However, the situation that there is no intensity change between the two consecutive pixels should also be considered and taken into account during pattern calculation. In this study, besides the intensity changes, we also consider the steady state where $\nabla = 0$. Furthermore, a threshold value is defined to alleviate the effects of external factors such as noise. That is, intensity changes lower than the threshold value will be ignored and defined as the steady state. Besides, previously studies ordinarily consider the relationship between the reference pixel ($I_{i,j}$) and its successor ($I_{i,j+1}$) or predecessor ($I_{i,j-1}$) (for $\alpha = 0°$). However, a more discriminative descriptor is achieved by considering the relationship between the reference pixel and both its predecessor and successor pixels. Thus, nine alternative patterns emerge as a result of this multi-state relationship consideration. Multi-valued (ternary) representation is utilized to handle this large number of states. The applied encoding methodology for 1-hop neighborhood is as follows:

Let, I_n is the intensity value of the reference pixel, and I^{α}_{n-1}, I^{α}_{n+1} denote the intensity values of the predecessor and successor pixels in the specified direction (α) respectively,

$$\nabla^{s,\alpha}_{n} = I^{\alpha}_{n+1} - In - thr \tag{24}$$

$$\nabla^{p,\alpha}_{n} = I^{\alpha}_{n-1} - In - thr \tag{25}$$

Table 1 Multi-valued codes depending on the value of ∇

$\nabla_n^{s,\alpha}$	$\nabla_n^{p,\alpha}$	Code	$\nabla_n^{s,\alpha}$	$\nabla_n^{p,\alpha}$	Code
↓	↓	00	→	↑	12
↓	→	01	↑	↓	20
↓	↑	02	↑	→	21
→	↓	10	↑	↑	22
→	→	11			

where $\nabla_n^{s,\alpha}$ and $\nabla_n^{p,\alpha}$ denote the gradient values through angle α respectively. The corresponding multi-valued pattern for the specified direction is defined according to Table 1:where →, ↑, ↓ denote 0, positive and negative gradients respectively. Multi-valued codes ($C_{i,j}^{\alpha}$) for each direction, namely, $\alpha = 0°$, *45°, 90°*, *135°*, *180°*, *225°*, *275°* and *315°* are calculated according to Table 1. Following this, the ultimate multi-valued pixel code (pixcode) $C_{i,j}^{k,thr}$ is defined by addition of the eight distinct $C_{i,j}^{\alpha}$ in radix *3*.

$$C_{i,j}^{k,thr} = C_{i,j}^{0°}(+)3\ C_{i,j}^{45°}\ (+)3\ \ C_{i,j}^{90°}\ (+)3\ C_{i,j}^{135°}\ (+)3\ C_{i,j}^{180°}\ (+)3\ C_{i,j}^{225°}\ (+)3\ C_{i,j}^{270°}\ (+)3\ C_{i,j}^{315°} \tag{26}$$

where $(+)_3$ stands for the arithmetic addition operation in radix *3* and of which the truth table is given below:

X/Y	0	1	2
0	0	1	2
1	1	2	0
2	2	0	1

3.3 Back-to-binary conversion and scaling

The basic LBP and some of its variants do only consider the relationship between the reference pixel and its neighbors. However, the information concealed in the magnitude of the difference is being discarded in this way. Because of that, it is possible to arise the challenge of two pixels with different intensities having identical values in the new domain. The most proficient way of handling this situation is to take into account the value of the reference pixel by scaling the resulting decimal pixcode value by the intensity value of the reference pixel. Figure 7 illustrates the challenge of having the same binary patterns for pixels with different intensities and how our method handles this situation.

In DLGBD, the next step after calculation of pixcodes is the conversion and scaling of those multi-valued pixcodes to *uint8* type values in order to maintain operations in the 8-bit gray-scale domain. The conversion of pixcodes back to the 8-bit grayscale domain is done as follows:

$$B_{C_{i,j}^{k,thr}} = \left(\sum_{l=0}^{l=D-1} D_l \times r^{l-1}\right) \times \left(I_{i,j}\right) \times (255/2040) \tag{27}$$

where r denotes the radix. *255* is the maximum gray-level intensity value and *2040* is the maximum value that can be calculated as the result of multiplication of the maximum two-digit ternary number $(22)_3$ and 255. These values are used to scale the result into the interval [0–255] and find the ultimate DGBLD(i,j).

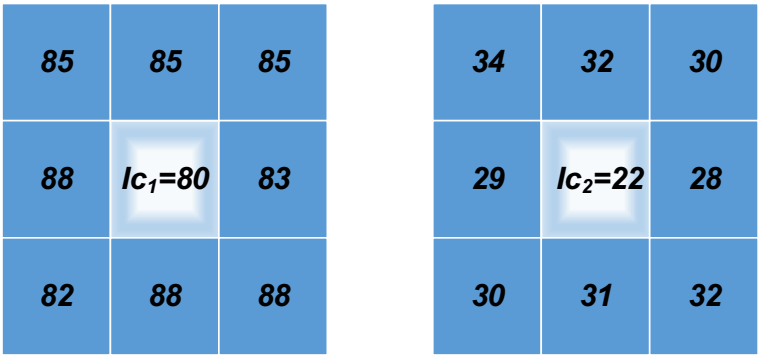

Fig. 7 **a** Identical LBP codes assigned to different patterns **b** The proposed descriptor overcomes the miss-assignment situation

Figure 8 illustrates the applied methodology on a sample sub-region of an image for 1-hop neighborhood:

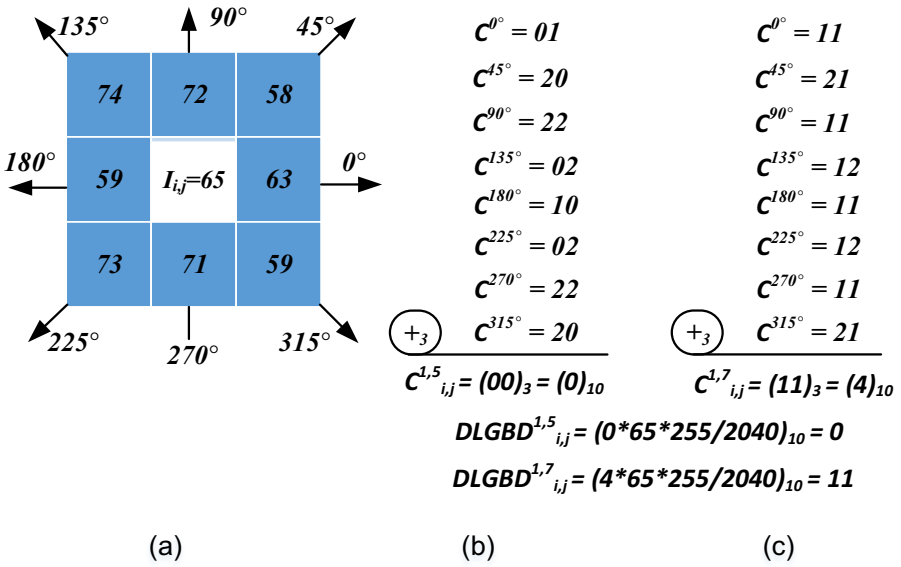

$$C^{k,thr}_{i,j} = C^{0^\circ} \overset{+_3}{} C^{45^\circ} \overset{+_3}{} C^{90^\circ} \overset{+_3}{} C^{135^\circ} \overset{+_3}{} C^{180^\circ} \overset{+_3}{} C^{225^\circ} \overset{+_3}{} C^{270^\circ} \overset{+_3}{} C^{315^\circ}$$

$$DLGBD^{k,thr}_{i,j} = I_{i,j} * C^{k,thr}_{i,j}$$

Fig. 8 **a** Sample image matrix **b** $C^{1,5}_{i,j}$, *1-hop* pixcode for *thr* = 5 **c** $C^{1,7}_{i,j}$, *1-hop* pixcode for *thr* = 7

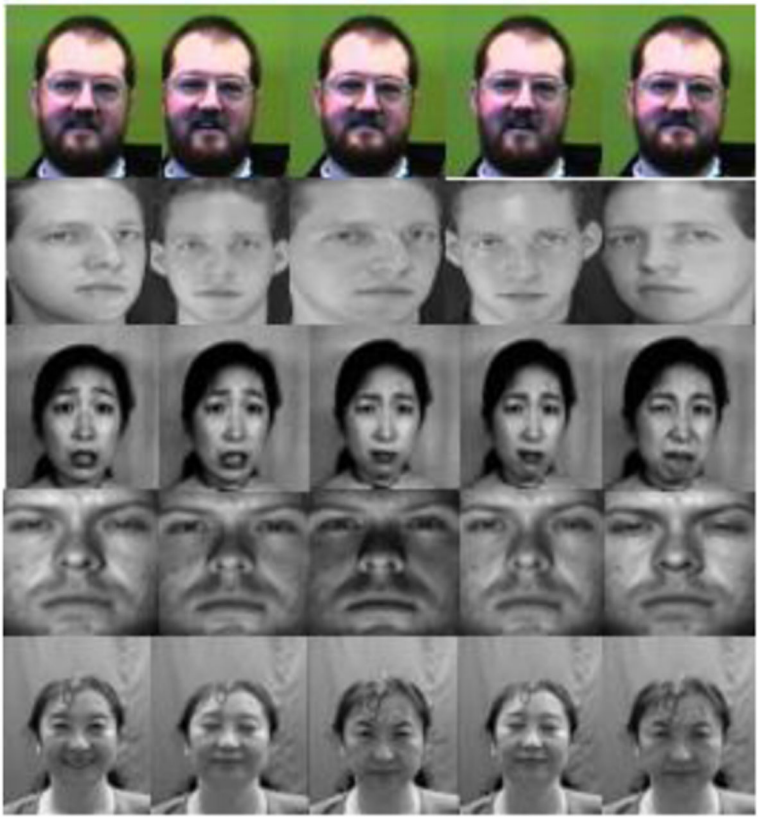

Fig. 9 Examples of face images extracted from Face94, ORL, JAFFE, Yale and CAS-PEAL-R1 databases respectively

4 Experimental results

Several experiments are conducted to evaluate and compare the performance of DLGBD with the against a number of state-of-the-art methods on the face recognition task using five benchmark databases, namely Face94 [29], ORL [48] JAFFE [32], Yale (http://vision.ucsd.edu/content/yale-face-database). Sample images retrieved from the mentioned databases are presented in Fig. 9.

Some preprocessing operations are applied to each image to provide the uniformity. Each image is firstly scaled to the size 64×64. Following the scaling stage, to eliminate the effect of redundant background and foreground factors, the face extraction is done by using the Viola Jones [57] algorithm.

The performance analysis of the proposed framework is performed in two folds. In the first step, the stability and resistance of the method against rotational, illumination changes and noise effects are clarified. Later, the recognition performance of the proposed method is analyzed and compared to the the-state-of-art methods such as LBP, LDP, LDNP (Local Directional Number Pattern), Gabor Features, HoG (Histogram of Gradients), LTP, LTetP (Local Tetra Pattern) [52] and LDrvP (Local Derivative Pattern) [61] by conducting extensive simulations. Experiments are executed on MATLAB 2017b running on the computer system with the specifications Intel CORE i7-5500 U 2.4 GHz processor and 8 GB RAM.

4.1 The stability analysis

As mentioned previously, rotational changes, variation of illumination and noise significantly affect the recognition performance. Thus, the proposed local descriptor and the overall architecture should not fail under challenging circumstances and keep robust in order to accomplish the recognition task satisfactorily. In advance, it is illustrated how the proposed local descriptor stands robustly against the rotational changes. Following this, the performance analysis is conducted to verify the resistance of DLGBD against illumination variations by extensive simulations. The last part in this section demonstrates the analysis results of the simulations done to see the behavior of DLGBD under varying noisy circumstances.

4.1.1 Rotation-variation resistance analysis

A robust texture descriptor should behave stable and produce similar features even the original image is rotated, because the content of the image does not change and it belongs to the same individual. Thus, it is important to show and verify the behavior of the proposed method when the image is suffered to rotational variations. Figure 10 depicts the stability performance of DLGBD. In Fig. 10, a sample matrix, which symbolizes a block of an image is demonstrated. As depicted in the figure, the local descriptor content that is extracted from the block does not change even the matrix is rotated 90° counter clockwise.

The rotation resistance performance analysis of DLGBD is done and compared to the other methods in two-folds. Firstly, without any training, similarity analysis is done by examining the chisq distances between the rotated image of an individual and the remaining images of the same individual. During the search stage, if the image, that has the minimum chisq distance with the rotated image, belongs to the same individual, then a true-positive situation occurs (a

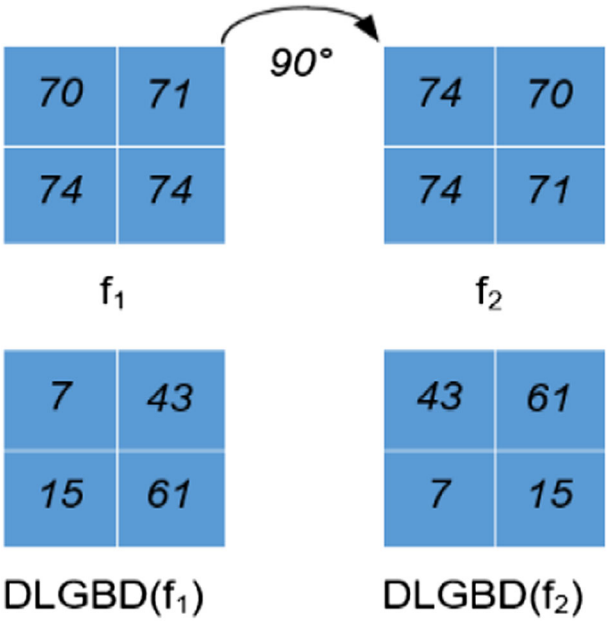

Fig. 10 Illustration of the robustness of DLGBD against rotational changes on a sample matrix

Table 2 The matching rates by considering the similarities without any training (TP, FP refers to the TruePositive and FalsePositive respectively)

Method	Accuracies							
	Face94		CAS-PEAL-R1		JAFFE		ORL	
	TP	FP	TP	FP	TP	FP	TP	FP
DLGBD	91	2	179	198	7	3	33	7
LTrnP	92	1	218	159	8	2	32	8
LDNP	5	88	1	377	0	10	4	36
LDrvP	0	93	2	375	0	10	2	38
LDP	9	84	0	377	0	10	5	35
LBP	0	93	0	377	0	10	2	38
LTetP	23	70	0	377	0	10	1	39
Gabor	1	92	0	377	0	10	5	35
HoG	62	31	0	377	4	6	6	34

hit state). On the contrary, if labels of the matched image and the image being searched are not identical then a false-positive situation occurs (a miss state). Table 2 gives the results of matching rates belonging to DLGBD and other methods, on different databases. Obviously, DLGBD performs far better than any other method in terms of finding the right face without training.

In the second step, the face recognition performance analysis is done by committing training for each method on each database. During the training phase, half of the training data is rotated and given to the training algorithm. By this way, the system is being trained by both the rotated and non-rotated images of the individuals and intended to match a rotated test image with the correct individual. Table 3 clarifies the classification results of DLGBD and other methods as a result of supervised training. Again, DLGBD shows promising performance in terms of recognition accuracy even under the circumstance of rotational variation.

4.1.2 Noise resistance analysis

The second important factor that affects the recognition performance of a method is the noise. In order for a method to be considered as high performance in terms of face recognition

Table 3 The classification accuracy performances as the result of supervised training

Method	Accuracies				
	Face94	YALE	CAS-PEAL-R1	JAFFE	ORL
DLGBD	1,000	0,826	0,812	0,960	0,825
LTrnP	0,991	0,771	0,846	0,960	0,550
LDNP	0,996	0,779	0,809	0,960	0,675
LDrvP	0,991	0,696	0,737	0,880	0,450
LDP	0,991	0,693	0,711	0,940	0,450
LBP	1,000	0,712	0,844	0,900	0,575
LTetP	0,998	0,594	0,751	0,800	0,588
Gabor	1,000	0,720	0,812	0,900	0,725
HoG	1,000	0,820	0,971	0,980	0,788

Table 4 The values of correlation between the feature sets of salt-pepper noisy and non-noisy images

Method	Correlation (feature sets)				
	Face94	YALE	CAS-PEAL-R1	JAFFE	ORL
DLGBD	0,889	0,811	0,741	0,759	0,827
LTrnP	0,804	0,817	0,809	0,761	0,806
LDNP	0,040	0,010	0,010	0,010	0,010
LDrvP	0,010	0,258	0,399	0,332	0,010
LDP	0,384	0,453	0,477	0,439	0,416
LBP	0,787	0,878	0,940	0,916	0,927
LTetP	0,990	0,990	0,990	0,990	0,990
Gabor	0,970	0,982	0,938	0,990	0,860
HoG	0,837	0,611	0,604	0,649	0,560

accuracy, it must be able to react strongly to the noise factor and not be affected by noise. As have been done in previous studies that have been proposed thus far, the salt-pepper and Gaussian noise have been applied artificially on the images on each database. Following, the similarity analysis is done between the original and noisy images of an individual on each database. The similarity analysis is done by examining the correlation between feature sets of the salt-pepper noisy and non-noisy versions of the face images. Also, as a second step of salt-pepper noise effect analysis is done by investigating the correlation between the histograms of the feature sets belonging to the noisy and non-noisy images.

The second noise resistance analysis is made upon involving the Gaussian noise. The Gaussian noise with different variance (σ^2) values are exposed to the images in each dataset. As in the salt-pepper noise effect analysis, the similarity and correlation values are measured between the images and their Gaussian noise suffered versions. As clearly expressed by Tables 4, 5, 6 and 7, the similarity between the histograms of the noisy-image-feature sets and non-noisy-image-feature sets that are produced by DLGBD are high when compared to the other methods. This proves the robustness of DLGBD against noise such as salt-pepper and Gaussian.

Table 5 The values of correlation between the histograms of the feature sets of salt-pepper noisy and non-noisy images

Method	Correlation (feature sets)				
	Face94	YALE	CAS-PEAL-R1	JAFFE	ORL
DLGBD	0,984	0,916	0,905	0,913	0,920
LTrnP	0,988	0,986	0,988	0,988	0,989
LDNP	0,963	0,976	0,803	0,935	0,981
LDrvP	0,988	0,988	0,989	0,989	0,990
LDP	0,010	0,868	0,880	0,894	0,938
LBP	0,700	0,852	0,740	0,810	0,931
LTetP	0,990	0,990	0,990	0,990	0,990
Gabor	0,808	0,656	0,910	0,975	0,821
HoG	0,819	0,010	0,913	0,980	0,900

Table 6 The MSE values between the feature set of a non-noisy image (CASPEALR1) and feature sets of its Gaussian noisy versions

Method	σ2 = 0.01	σ2 = 0.02	σ2 = 0.03	σ2 = 0.04	σ2 = 0.05
DLGBD	0,010	0,511	0,552	0,767	0,990
LTrnP	0,010	0,563	0,951	0,970	0,990
LDNP	0,010	0,538	0,832	0,945	0,990
LDrvP	0,010	0,276	0,544	0,786	0,990
LDP	0,010	0,334	0,908	0,951	0,990
LBP	0,010	0,558	0,801	0,957	0,990
LTetP	0,010	0,574	0,715	0,740	0,990
Gabor	0,010	0,219	0,506	0,743	0,990
HoG	0,010	0,320	0,706	0,990	0,986

Table 7 The correlation values between the feature set of a non-noisy image (CASPEALR1) and feature sets of its Gaussian noisy versions

Method	σ2 = 0.01	σ2 = 0.02	σ2 = 0.03	σ2 = 0.04	σ2 = 0.05
DLGBD	0,701	0,622	0,621	0,594	0,552
LTrnP	0,313	0,260	0,223	0,215	0,221
LDNP	0,464	0,342	0,282	0,191	0,196
LDrvP	0,728	0,561	0,502	0,462	0,407
LDP	0,309	0,232	0,199	0,178	0,139
LBP	0,400	0,350	0,346	0,334	0,319
LTetP	0,720	0,672	0,653	0,624	0,631
Gabor	0,995	0,986	0,965	0,963	0,946
HoG	0,955	0,891	0,919	0,852	0,843

4.2 The recognition performance analysis

In order to accurately measure and analyze the performance of the proposed framework and compare to the state-of-the-art methods in the area, the hold out testing is utilized. That is, if there are N images of an individual in a dataset, %80 of these and the average image of them are used for training. The rest are used for testing. While forming the average face image, the images of each individual are inherently aligned by considering the eyes of the individual. An exemplary average face calculation of an individual is given in Fig. 11:

Fig. 11 Sample face images of an individual and his average face image

Table 8 The recognition performance results regarding supervised training

Method	Face94	YALE	CAS-PEAL-R1	JAFFE	ORL
DLGBD	1,000	0,949	0,963	1,000	0,925
LTrnP	0,991	0,941	0,947	1,000	0,775
LDNP	0,996	0,943	0,950	1,000	0,750
LDrvP	0,991	0,946	0,889	0,900	0,638
LDP	0,991	0,939	0,881	0,980	0,725
LBP	1,000	0,907	0,912	0,960	0,825
LTetP	0,998	0,905	0,836	0,780	0,725
Gabor	1,000	0,913	0,897	0,820	0,863
HoG	1,000	0,916	0,995	1,000	0,888

The recognition performance analysis of DLGBD is done in two ways: 1- Training-based recognition performance analysis 2- Similarity-based recognition performance analysis.

4.2.1 Training-based recognition performance analysis

At this stage, the supervised learning method has been utilized while classifying. %80 of each individual in each dataset is used for training and the remaining images of the individuals are utilized for testing. Table 8 shows the performance results of DLGBD and the-state-of-the-art methods in terms of recognition accuracy. As it can be seen in Table 8, DLGBD performs promisingly well when compared to other methods in terms of classification accuracy analysis using supervised learning. DLGBD performs remarkably even on the challenging datasets CAS-PEAL-R1, JAFFE and ORL.

4.2.2 Similarity-based recognition performance analysis

At this stage, recognition performance of DLGBD and the-state-of-the art methods are done by implementing similarity analysis between the feature sets of the images. That is, the feature set of the image that is being searched is calculated and then compared to the feature sets of each image in the dataset. If the tag of the most similar image

Table 9 The recognition performance results regarding similarity analysis

Method	Accuracies							
	Face94		CAS-PEAL-R1		JAFFE		ORL	
	TP	FP	TP	FP	TP	FP	TP	FP
DLGBD	93	0	291	86	8	2	36	4
LTrnP	85	8	208	169	8	2	16	24
LDNP	93	0	270	107	9	1	29	11
LDrvP	77	16	144	233	7	3	19	21
LDP	62	31	150	227	4	6	11	29
LBP	24	69	19	358	1	9	5	35
LTetP	21	72	53	324	10	0	38	2
Gabor	93	0	68	309	10	0	40	0
HoG	93	0	49	328	10	0	40	0

found matches up with the tag of the image that is being searched, that shows a hit (true-positive), otherwise a miss (false-positive). Table 9 figures out the recognition accuracy performances of each method on each dataset. As clarified in the table, DLGBD competes with the other methods even on the challenging datasets without any training that is without any knowledge.

5 Conclusion

In this paper, a novel Directional Local Gradient Based Descriptor (DLGBD) for image retrieval is presented. The proposed method extracts local gradient-based patterns in terms of direction-dependent neighbors. The relations between the pixels are handled in four directions. The local neighborhood comprises the pixels at most k-hop away. The population of the neighborhood differs due to the value of k. The neighbors of a reference pixel are categorized according to their angular position relative to that pixel. Since using larger number of threshold values increases the computational cost of the algorithm and at the same time it does not preserve the high recognition rates we used threshold value not more than five. The experimental results demonstrate that the proposed descriptor achieves promising scores and outperforms the state-of-art methods in terms of classification accuracy. Besides its favorable recognition performance, DLGBD also handles the effects of rotational variances and noise affects very successfully when compared to the state-of-the-art methods. As a future work, it is intended to examine how multi-spectral evaluation and dynamic neighborhood size depending on some criteria can contribute to the recognition performance of the method.

References

1. Ahonen T, Hadid A, Pietikainen M (2004) Face recognition with local binary patterns. In: Proceedings of the 8th European Conference on Computer Vision, pp. 469–481
2. Ahonen T, Hadid A, Pietikainen M (2006) Face recognition with local binary patterns: Application to Face Recognition. IEEE Trans Pattern Anal Mach Intell 28(12):2037–2041
3. Bo Y, Chen S A Comparative Study on Local Binary Pattern (LBP) based face recognition: LBP Histogram versus LBP Image. Neurocomputing 120:365–379
4. Chakraborty S (2017) Satish Kumar Singh, Pa-van Chakraborty, "Local Directional Gradient Pat-tern: a Local Descriptor for Face Recognition". Multimedia Tools and Applications 76:1201–1216
5. Chakraborty S, Singh SK, Chakraborty P-v (2016) Local Gradient Hexa Pattern: A Descriptor for Face Recognition and Retrieval. IEEE Transactions on Circuits and Systems for Video Technology PP(99):1–1
6. Chen X, Zhang JS (2010) Maximum variance difference based embedding approach for facial feature extraction. Int J Pattern Recognit Artif Intell 24(7):1–14
7. Dahmane M, Meunier J (2011) Emotion recognition using dynamic gridbased HoG features. In: IEEE Int. Conf. Autom. Face Gesture Recognit. Workshops (FG), pp. 884–888
8. Dan Z, Chen Y, Yang Z, Wu G (2014) An Improved Local Binary Pattern for Texture Classification. Optik 125:6320–6324
9. Doshi N, Schaefer G (2012) A comprehensive benchmark of local binary pattern algorithms for texture retrieval. Proceedings of the International Conference on Pattern Recognition (ICPR), pp. 2760–2763
10. Dubey SR (2017) Local directional relation pattern for unconstrained and robust face retrieval. arXiv: 1709.09518 [cs.CV]
11. Etemad K, Chellappa R (1997) Discriminant Analysis for recognition of human face images. J Opt Soc Am A 14(8):1724–1733

12. Fan KC, Hung TY (2014) A novel local patterndescriptor-local vector pattern in high-order derivative space for face recognition. IEEE Trans Image Process 23(7):2877–2891
13. Fernández A, Álvarez M, Bianconi F (2013) Texture description through histograms of equivalent patterns. J Math Imaging Vis 45(1):76–102
14. Guan Z, Wang C, Chen Z, Bu J, Chen C (2010) Efficient Face Recognition Using Tensor Subspace Regression. Neurocomputing 73:2744–2753
15. Haralick RM (1979) Statistical and structural approach to texture. Proc IEEE 67(5):786–804
16. Haralick RM, Shanmugan K, Dinstein I (1973) Textural features for image classification. IEEE Transactions on Systems, Man and Cybernetics 3:610–621
17. Heikkilä M, Pietikäinen M, Schmid C (2009) Description of interest regions with local binary patterns. Pattern Recogn 42(3):425–436
18. Huang D, Shan C, Ardabilian M, Wang Y, Chen L (2011) Local binary patterns and its application to facial image analysis: a survey. IEEE Trans Syst Man Cybern—Part C: Appl Rev 41(6):765–781
19. Jabid T, Kabir MH, Chae O (2010) Robust facial expression recognition based on local directional pattern. ETRI J 32(5):784–794
20. Jafari-Khouzani K, Soltanian-Zadeh H (2005) Radon transform orientation estimation for rotation invariant texture analysis. IEEE Trans Pattern Anal Mach Intell 27(6):1004–1008
21. Jafri R, Arabnia HR (2009) A Survey of Face Recognition Techniques. Journal of Information Processing Systems 5(2):41–68
22. Jain A, Hong L, Pankanti S (2000) Biometric Identification. Commun ACM 43(2):91–98. https://doi.org/10.1145/328236.328110
23. Jain AK, Ross A (2008) Introduction to biometrics. In: Jain AK; Flynn, Ross A. (eds) Handbook of Biometrics. Springer, pp. 1–22. ISBN 978–0–387-71040-2
24. Kellokumpu V, Zhao G, Pietikäinen M (2008) Human activity recognition using a dynamic texture based method. Proceedings of the British Machine Vision Conference
25. Kirby M, Sirovich L (1990) Applications of the Karhunen–Loeve procedure for the characterisation of human faces. IEEE Trans Pattern Anal Mach Intell 12:103–108
26. Lazebnik S, Schmid C, Ponce J (2005) A sparse texture representation using local affine regions. IEEE Trans Pattern Anal Mach Intell 27(8):1265–1278
27. Lei Z, Liao S, Pietikainen M (2011) Face Recognition by Exploring Information jointly in Space, Scale, and Orientation. IEEE Trans Image Process 20(1):247–256
28. Lei Z, Liao S, Pietikäinen M, Li SZ (2011) Face recognition by exploring information jointly in space, scale and orientation. IEEE Trans Image Process 20(1):247–256
29. Libor S (2000) Face recognition data
30. Liu L, Fieguth P, Guo Y, Wang X, Pietikainen M (2017) Local Binary Features for Texture Classification: Taxonomy and experimental study. Pattern Recogn 62:135–160
31. Liu L, Long Y, Fieguth PW, Lao S, Zhao G (2014) BRINT: Binary Rotation Invariant and Noise Tolerant Texture Classification. IEEE Trans Image Process 23(7):3071–3084
32. Lyons MJ, Akemastu S, Kamachi M, Gyoba J (1998) Coding Facial Expressions with Gabor Wavelet. 3rd IEEE International Conference on Automatic Face and Gesture Recognition, pp. 200–205
33. Melendez J, Garcia MA, Puig D (2008) Efficient distance-based per-pixel texture classification with Gabor wavelet filters. Pattern Anal Applic 11(3):365–372
34. Nanni L, Brahnam S, Ghidoni S, Menegatti E, Barrier T (2013) Different Approaches for Extracting Information from the Co-Occurrence Matrix. PLoS One 8(12):1–9
35. Nanni L, Brahnam S, Lumini A (2010) A local approach based on a local binary patterns variant texture descriptor for classifying pain states. Expert Syst Appl 37(12):7888–7894
36. Nanni L, Lumini A, Brahnam S (2010) Local binary patterns variants as texture descriptors for medical image analysis. Artif Intell Med 49(2):117–125
37. Nanni L, Lumini A, Brahnam S (2012) Survey on lbp based texture descriptors for image classification. Expert Syst Appl 39(3):3634–3641
38. Nisenson M, Yariv I, El-Yaniv R, Meir R (2003) Towards behaviometric security systems: learning to identify a typist. Lecture Notes in Computer Science, pp. 363–374
39. Ojala T, Pietikäinen M, Harwood D (1996) A comparative study of texture measures with classification based on feature distributions. Pattern Recogn 29(1):51–59
40. Ojala T, Pietikäinen M, Mäenpää T (2002) Multiresolution gray-scale and rotation invariant texture classification with local binary patterns. IEEE Trans Patterns Anal Mach Intell 24(7):971–987
41. Pietikäinen M, Hadid A, Zhao G, Ahonen T (2011) Computer vision using local binary patterns. Computational Imaging and Vision
42. Pietikäinen M, Ojala T, Xu Z (2000) Rotation-invariant texture classification using feature distributions. Pattern Recogn 33(1):43–52

43. Qi X, Xiao R, Li C-G, Qiao Y, Guo J, Tang X (2014) Pairwise Rotation Invariant Co-occurrence Local Binary Pattern. IEEE Trans Pattern Anal Mach Intell 36(11):2199–2213
44. Qian X, Hua X-S, Chen P, Ke L (2011) PLBP: An Effective Local Binary Patterns Texture Descriptor with pyramid represenation. Pattern Recogn 44:2502–2515
45. Ramirez Rivera A, Castillo R, Chae O (2013) Local directional number pattern for face analysis: Face and expression recognition. IEEE Trans Image Process 22(5):1740–1752
46. Rivera AR, Castillo JR, Chae O (2013) Local directional number pattern for face analysis: face and expression recognition. IEEE Trans Image Process 22(5):1740–1752
47. Rivera AR, Chae O (2015) Spatiotemporal directional number transitional graph for dynamic texture recognition. IEEE Trans Pattern Anal Mach Intell 37(10):2146–2152
48. Sarasota FL (1994) Proceedings of 2nd IEEE Workshop on Applications of Computer Vision
49. Satpathy A, Jiang X, Eng H (2014) Lbp based edge texture features for object recognition. IEEE Trans Image Process 23(5):1953–1964
50. Saul LK, Roweis ST (2003) Think globally, fit locally: unsupervised learning of low dimensional manifolds. The Journal of Machine Learning Research 4:119–155
51. Silven O, Niskanen M, Kauppinen H (2003) Wood inspection with nonsupervised clustering. Mach Vis Appl 13:275–285
52. Subrahmanyam Murala RP, Maheshwari RB (2012) Local Tetra Patterns: A New Feature Descriptor for Content-Based Image Retrieval. IEEE Trans Image Process 21(5):2874–2886
53. Tan X, Triggs B (2010) Enhanced local texture feature sets for face recognition under difficult lighting conditions. IEEE Trans Image Process 19(6):1635–1650
54. Trefny J, Matas J (2010) Extended set of local binary patterns for rapid object detection. Proceedings of the Computer Vision Winter Workshop
55. Turk MA, Pentland AP (1991) Eigenfaces for Recognition. J Cogn Neurosci 3(1):71–86
56. Varma M, Zisserman A (2009) A statistical approach to material classification using image patch exemplars. IEEE Trans Pattern Anal Mach Intell 31(11):2032–2047
57. Viola P, Jones MJ (2004) Robust real-time face detection. Int J Comput Vis 57:137–154
58. Yang S, Bhanu B (2011) Facial expression recognition using emotion avatar image. In: IEEE Int. Conf. Autom. Face Gesture Recognit. Workshops (FG), pp. 866–871
59. Yang J, Zhang D, Frangi AF, Yang J (2004) PCA Two-dimensional, a new approach to appearance-based face representation and recognition. IEEE Trans Pattern Anal Mach Intell 26(1):131–137
60. Yin QB, Kim JN (2008) Rotation-invariant texture classification using circular Gabor wavelets based local and global features. Chin J Electron 17(4):646–648
61. Zhang B, Gao Y, Zhao S, Liu J (2010) Local Derivative Pattern Versus Local Binary Pattern: Face Recognition with High-Order Local Pattern Descriptor. IEEE Trans Image Process 19(2):533–543
62. Zhang B, Shan S, Chen X, Gao W (2007) Histogram of gabor phase patterns (hgpp): A novel object representation approach for face recognition. IEEE Trans Image Process 16(1):57–68
63. Zhang WC, Shan SG, Gao W, Zhang HM (2005) Local gabor binary pattern histogram sequence (LGBPHS): a novel non-statistical model for face representation and recognition. In: Proceedings of the 10th IEEE International Conference and Computer Vision, pp. 786–791
64. Zhao G, Pietikäinen M (2007) Dynamic texture recognition using local binary patterns with an application to facial expressions. IEEE Trans Pattern Anal Mach Intell 29(6):915–928
65. Zhong F, Zhang J (2013) Face Recognition with Enhanced Local Directional Patterns. Neurocomputing 119:375–384

Nazife Cevik She obtained the PhD. degree from Istanbul University in 2012. She joined the Computer Engineering Department at Istanbul Arel University in 2015 and continues to work as an Assistant Professor. Her research interests are Image Processing, Machine Learning and Bioinformatics. Mailing Address: Istanbul Arel University Tepekent Department of Computer Engineering Büyükçekmece Istanbul Turkey. Email Address: nazifecevik@arel.edu.tr

Taner Cevik He received the B.Sc. degree in computer engineering from Istanbul Technical University, Istanbul in 2001, and obtained his Master of Science degree in computer engineering from Fatih University, Istanbul in 2008. Following, completed Ph.D. at Istanbul University in 2012. He joined the Sortware Engineering Department at Aydin University in 2017 and continues to work as an Associate Professor. His research interests are Image Processing and Wireless Multimedia Sensor Networks. Mailing Address: Ataturk Mahallesi, Gazi Mustafa Kemal Caddesi Deran Sokak No: 6/5 Büyükçekmece Istanbul Turkey. Email Address: tanercevik@aydin.edu.tr